VILNIUS TECH
Vilnius Gediminas Technical University

Geodesy and Cartography
ISSN 2029-6991 / eISSN 2029-7009
2022 Volume 48 Issue 3: 134–143
https://doi.org/10.3846/gac.2022.16215

UDC 528.714

CALIBRATION OF THE LOW-COST UAV CAMERA ON A SPATIAL TEST FIELD

Szymon SOBURA*

Department of Geodesy and Geomatics, Faculty of Environmental, Geomatic and Energy Engineering, Kielce University of Technology, Kielce, Poland

Received 30 December 2021; accepted 02 September 2022

Abstract. For several years, the widening range of applications of unmanned aerial vehicles can be noticed not only in the literature review but also in the market of services offered – also in the geodetic sector. While there is a wide range of professional UAVs for aerial mapping tasks, these platforms are expensive. In this study, it was checked whether the calibration of a low-cost drone camera allows for obtaining an accuracy acceptable for photogrammetric studies. For this purpose, a spatial test field was designed on which a multivariate calibration of the UAV camera and control of the obtained results were carried out. Using the elements of the camera's internal orientation obtained during the calibration process, it was not possible to achieve high accuracy of photogrammetric measurements on control images. This may indicate a problem with the repeatability of determining the elements of internal orientation of the analyzed camera, and thus with the instability of the autofocus system. Nevertheless, the use of the obtained results from the camera calibration as precise approximations of the elements of the camera's internal orientation had a positive effect on the solution of the image network using the bundle adjustment and the fitting of the spatial model to the ground control points. In addition, the UAV flight over the created spatial test field allowed for a reliable assessment of the possibilities and accuracy that can be obtained on the basis of images from a low-cost drone.

Keywords: UAV, calibration camera, bundle adjustment, test field, self-calibration, photogrammetric measurements.

Introduction

For several years now, the widening range of applications for unmanned aerial vehicles has been noticeable not only in the literature review but also on the market of geodetic services. Some of the applications in the field of short-range photogrammetry, such as inventorying monuments, mapping urban areas or monitoring areas subject to natural hazards, require high accuracy and precision of the observations obtained (Wiącek, 2020). Unfortunately, and most often, non-professional cameras used in low-cost drones do not have the known elements of internal orientation and distortion parameters, which translates into the accuracy of photogrammetric measurements (Bakuła & Ostrowski, 2012). This problem was noticed by the creators of photogrammetric software for processing images from UAV (Unmanned Aerial Vehicle), who corrected the deficiency of parameters in the Brown model to correct geometric distortions created in the images (Wiącek, 2020).

The problem of calibrating non-metric cameras and the instability of the internal orientation elements of the camera has been investigated by Cramer et al. (2017). In their research, the authors showed that in some non-metric cameras the value of the fixed camera and the coordinates of the principal point can change in the range of several tens of microns, although the camera was not operated surgically. This may mean that the thermal conditions of the camera's operation may affect the stability of the internal orientation elements (IOE) of such a camera (Wiącek, 2020). In the work (Sampath et al., 2012), the authors emphasize that photogrammetric designs can be performed without knowing the camera calibration parameters (before the image aerotriangulation process), however, such an approach requires designing a denser network of measurement points – ground control points (GCP) and check points (CP) – which in turn affects the time-consuming and costly nature of such a solution. Research (Radford & Bevan, 2019) has proven that UAV-mounted non-metric cameras can be calibrated at a satisfactory level of accuracy. For this purpose, the authors suggest creating custom flight plans for calibration that make good use of known non-metric camera calibration

*Corresponding author. E-mail: *ssobura@tu.kielce.pl*

practices published in recent years (Fryskowska et al., 2016; Wiącek & Pyka, 2019). In turn, the work (Sampath et al., 2012) presents two methods of stationary camera calibration using coded targets placed on an aluminum cage and a rigid box, obtaining results that are satisfactory for the authors.

In order to adapt a non-metric digital camera to precise 2D / 3D measurements, it is necessary to carry out a procedure of checking the stability of the designated elements of the camera's internal orientation, and then calibrating such a sensor. The camera calibration process involves defining the vector geometry in the image space by precisely defining the camera constant c_k and the coordinates of the principal point. Additionally, parameters of the distribution of radial and tangential distortion are determined to eliminate image errors. The literature review distinguishes several methods of calibrating non-metric digital cameras (Sampath et al., 2012; Tokarczyk & Boroń, 2000; Aldelgawy & Abu-Qasmieh, 2021). In practice, there are two approaches to determining the elements of the camera's internal orientation: self-calibration during operation (with simultaneous alignment of images) and calibration outside the measurement process (while the stability of the camera structure ensures the transfer of camera parameters over time). Currently, the concept of self-calibration is more comprehensive and means a procedure for simultaneously determining not only the internal elements of the camera orientation, but also the external elements of the orientation, image errors and coordinates of the points measured in the images. Self-calibration is commonly used when determining the internal orientation elements of digital cameras such as COTS (Commercial of the Shelf) installed on board a UAV for the purpose of mapping areas (Sobura, 2021).

In order to calibrate the non-metric camera, series of images of the appropriate configuration are taken, on which the test field or its fragments are photographed (Tokarczyk & Boroń, 2000; Aldelgawy & Abu-Qasmieh, 2021). There are flat test fields – 2D and spatial fields – 3D. Flat fields (e.g. checkerboards) are simple in construction and give good results when the camera is to be adapted to work for short object distances. The limitation of the use of such a field is the percentage of the frame filling with the field image, which is low for larger object distances and which affects the accuracy of determining the elements of internal orientation (Sobura, 2021). The spatial 3D fields for the calibration of apparatus require an appropriate distribution of the signaled points and high accuracy of determining the geometric relations between these points. Examples of test fields used for camera calibration are presented in Figure 1.

In the literature review, we can find the results of research on spatial test fields for the calibration of UAV cameras. In Oniga et al. (2018), the authors calibrated the camera of a low-cost drone in several variants: at different flight altitudes and with the use of various images configurations. The obtained results indicate that conducting the UAV flight in a cross configuration allows for the improvement of camera calibration results. The authors (Pérez et al., 2011) point to the problem of the appropriate arrangement and measurement of the photogrammetric control network in closed rooms for the purpose of creating a spatial field for UAV calibration. In order to solve the problem, they performed field calibration of the UAV camera by designing an appropriate test field. The obtained results from the field calibration were compared with the results from the laboratory calibration of the tested camera, obtaining more accurate results of determining the elements of internal orientation of the analyzed camera.

The main purpose of the research presented in the paper was to check whether the calibration of the camera of the Mavic 2 Pro low-cost drone, carried out on the proprietary test field, allows obtaining the accuracy acceptable for photogrammetric studies. The intermediate goal was to evaluate various image configurations in terms of their suitability for the calibration of UAV cameras.

1. Study area

For the purpose of calibration of UAV cameras, which most often capture images on the height of 60–100 m of relative height AGL (ang. Above Ground Level), the criteria for the selection of the test site were defined, which would enable the implementation of the goal set at the beginning:

- The test field must be spatially differentiated,
- Ground control points and check points should be measured with an accuracy of mp_{XYZ} <20 mm,

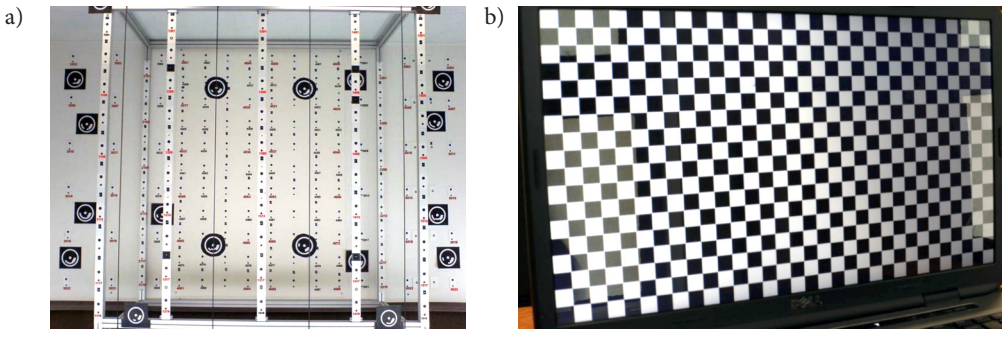

Figure 1. An example of the test fields used for the calibration of non-metric measurement cameras: a – a spatial test field at the Federal University of Technology in Zurich; b – a flat checkerboard test field in the Agisoft Lens software (source: Tokarczyk, 2022)

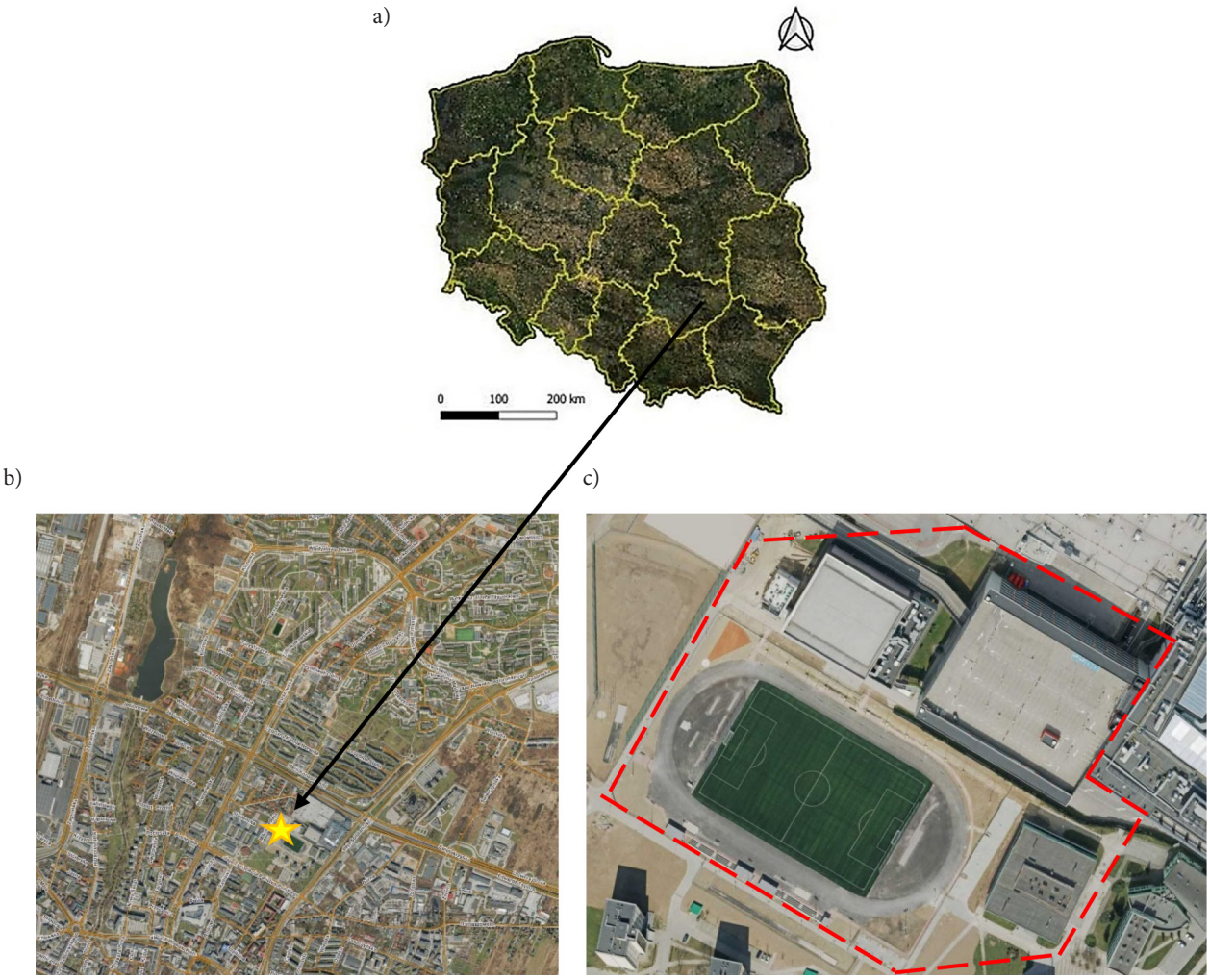

Figure 2. Location of the testing ground: a – approximate location against the background of Poland; b – general location of the athletics stadium in the eastern area of the city of Kielce, voivodeship Świętokrzyskie; c – detailed location of the training ground next to the Kielce University of Technology (Poland)

– The test field must have a large number of measured points in the form of well-defined field details,
– The distribution of image-points should be designed in such a way as to ensure that at least 5 image-points are photographed on each image obtained from the UAV,
– The forward and cross overlap coverage of the acquired images should not be less than 70%.

As the area that meets the above criteria, the area around the athletics stadium of the Kielce University of Technology and the multi-storey parking lot in Kielce (Poland), shown in Figure 2c, was selected. The separated section features a large number of field details in the form of sewage chambers and horizontal road signs, which made it possible to use these details as an unsigned photogrammetric image-points. The area of the test site was 5.5 ha, which made it possible to obtain images with the planned coverage at the altitude of 85 m AGL relative height during less than 20 minutes of flight with the UAV platform.

2. Methodology

2.1. Theoretical basics

The self-calibration procedure presented in the research is based on the use of the least squares method in the solution of simultaneous photogrammetric resection and intersection. The mathematical model of the collinearity equation is shown in Eq. (1):

$$x' - c_x = -c_k \frac{r_{11}(X - X_0) + r_{21}(Y - Y_0) + r_{31}(Z - Z_0)}{r_{13}(X - X_0) + r_{23}(Y - Y_0) + r_{33}(Z - Z_0)};$$

$$y' - c_y = -c_k \frac{r_{12}(X - X_0) + r_{22}(Y - Y_0) + r_{32}(Z - Z_0)}{r_{13}(X - X_0) + r_{23}(Y - Y_0) + r_{33}(Z - Z_0)}. \quad (1)$$

In the Equation (1) shown, the x' and y' coordinates are measured image coordinates. The parameters c_x and c_y define the coordinates of the principal point in the pixel coordinate system of the image. The parameter c_k is the camera constant determined in the calibration process, and the elements r_{11}–r_{33} contain the angular parameters

of the external orientation of the image at the time of its exposure. The collinearity equation connects image coordinates with terrain coordinates. It is a parametric and functional model, which means that additional conditions may be imposed on the presented equation to take into account optical aberrations, correction for atmospheric refraction or the curvature of the Earth.

One of the phenomena observed in the images is the non-linearity of straight lines caused by the distortion of the camera lens. Distortion in digital images is a systematic error, most often described by a polynomial. In Agisoft Metashape software, image errors (separated into Δx and Δy components) caused by distortion are calculated from Eq. (2):

$$\Delta x = x\left(1 + K_1 r^2 + K_2 r^4 + K_3 r^6 + K_4 r^8\right) + \left(P_1\left(r^2 + 2x^2\right) + 2P_2 xy\right)\left(1 + P_3 r^2 + P_4 r^4\right);$$

$$\Delta y = y\left(1 + K_1 r^2 + K_2 r^4 + K_3 r^6 + K_4 r^8\right) + \left(P_2\left(r^2 + 2y^2\right) + 2P_1 xy\right)\left(1 + P_3 r^2 + P_4 r^4\right). \quad (2)$$

Parameters $K_1 - K_4$ are the coefficients of radial distortion, $P_1 - P_4$ are the coefficients of tangential distortion, and the variables x and y are the coordinates of a point in the image, calculated on the basis of the formula 3 in the local matrix system of the camera. The local matrix coordinate system originates at the center of the camera projection. The X axis is clockwise, the Y axis is downward, and the Z axis is in the viewing direction (optical axis). To simplify the calculations, the X, Y, Z coordinates (from Eq. (3)) refer to the matrix origin, not the pixel image origin. In turn, the radial radius in the image is calculated in the Agisoft Metashape software using the Equation (4).

$$x = \frac{X}{Z}; \quad y = \frac{Y}{Z}; \quad (3)$$

$$r = \sqrt{\left(x^2 + y^2\right)}. \quad (4)$$

The final model of the collinearity equation with correction for image errors is presented in Eq. (5):

$$x' - c_x = -c_k \frac{r_{11}\left(X - X_0\right) + r_{21}\left(Y - Y_0\right) + r_{31}\left(Z - Z_0\right)}{r_{13}\left(X - X_0\right) + r_{23}\left(Y - Y_0\right) + r_{33}\left(Z - Z_0\right)} + \Delta x;$$

$$y' - c_y = -c_k \frac{r_{12}\left(X - X_0\right) + r_{22}\left(Y - Y_0\right) + r_{32}\left(Z - Z_0\right)}{r_{13}\left(X - X_0\right) + r_{23}\left(Y - Y_0\right) + r_{33}\left(Z - Z_0\right)} + \Delta y. \quad (5)$$

2.2. Characteristics of the test site and field work

On the test site presented in Figure 2b, 75 points were measured using the tachymetry method in the local coordinate system created for the purpose of the research. The limit mp_{XYZ} error in the position of the point in the local system was determined as mp_{XYZ} <20 mm. The error value resulted from the geometric resolution of the images from the Mavic 2 Pro unmanned aerial vehicle acquired at the height of 85 m AGL, which was 1.9 cm/pix. The declared flight altitude was selected empirically, based on the Authors' experiences in the implementation of other aviation tasks. Figure 3 shows the distribution of ground control points and check points inside the testing ground.

As image-points, both field details located within the testing ground were selected, as well as additional checkerboard targets and Maltese crosses were set up in places requiring the compaction of the photogrammetric image-points. The basic criterion allowing for the identification of a image-point with high precision is the high contrast of the point against the surroundings. For this reason, red spray markings have been made around some off-road details. Examples of image points used in the research are presented in Figure 4.

2.3. Workflow in research

All the preparatory and experimental work was divided into three main stages. As part of the first stage, image-points were designed and planned in the area of the testing ground around the Kielce University of Technology

Figure 3. Location of the distribution of ground control points and check points on the test site against the background of the generated cloud of points from the UAV in the Agisoft Metashape software

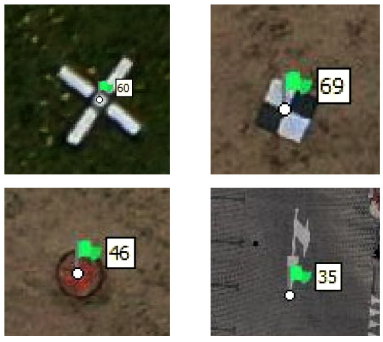

Figure 4. An example of signaling of image-points in the area of the testing ground – photogrammetric image-points signaled and not signaled on the obtained images from UAV

(Łojek & Łyjak, 2022). The second step was to collect image blocks of different configurations: almost vertical and oblique images. As part of the last stage, the acquired photogrammetric images were developed, determining the elements of the internal orientation of the UAV camera and carrying out controls of the obtained parameters. The adopted scheme of conduct in the research is presented in Figure 5.

3. Results

3.1. Calibration of the UAV camera

As part of the experimental work carried out, three flights with the DJI Mavic 2 Pro non-professional drone were carried out. The drone equipped with a camera with a 1″ CMOS matrix obtained a series of images with a resolution of 5472×3648 pixels. The Pix4D Capture application was used to plan the photogrammetric UAV flight. The autofocus system was used to set the ck, triggered from the desktop when the drone was at an altitude of 85 m AGL. Then the autofocus was turned off and the images were taken in manual mode for a given exposure triangle for the entire aviation mission.

As a result of UAV flights, 139 vertical images and 174 oblique images (gimbal tilt 80°) were obtained with a terrain pixel of 1.9 cm/pix. Additionally, for the purposes of controlling the results, an additional series of 154 oblique images was obtained above the experimental field with a terrain pixel of 2.3 cm/pix. The self-calibration procedure with simultaneous aerotriangulation of the image block was performed in the Agisoft Metashape software. During the initial orientation of the images, attention was paid to the observations that differed from the other data, which resulted from measurement errors or a point that is difficult to detect. It was decided to remove uncertain observations. Consequently, out of 75 measured image-points, 60 GCP (Ground Control Points) were used for further calculations.

Figure 6 shows the distribution of model fitting errors on ground control points after aligning the image blocks in three configurations: vertical images, oblique images, vertical and oblique images. The size and direction of the error ellipse indicate the error after the XY components. The color of the ellipse per Z component error.

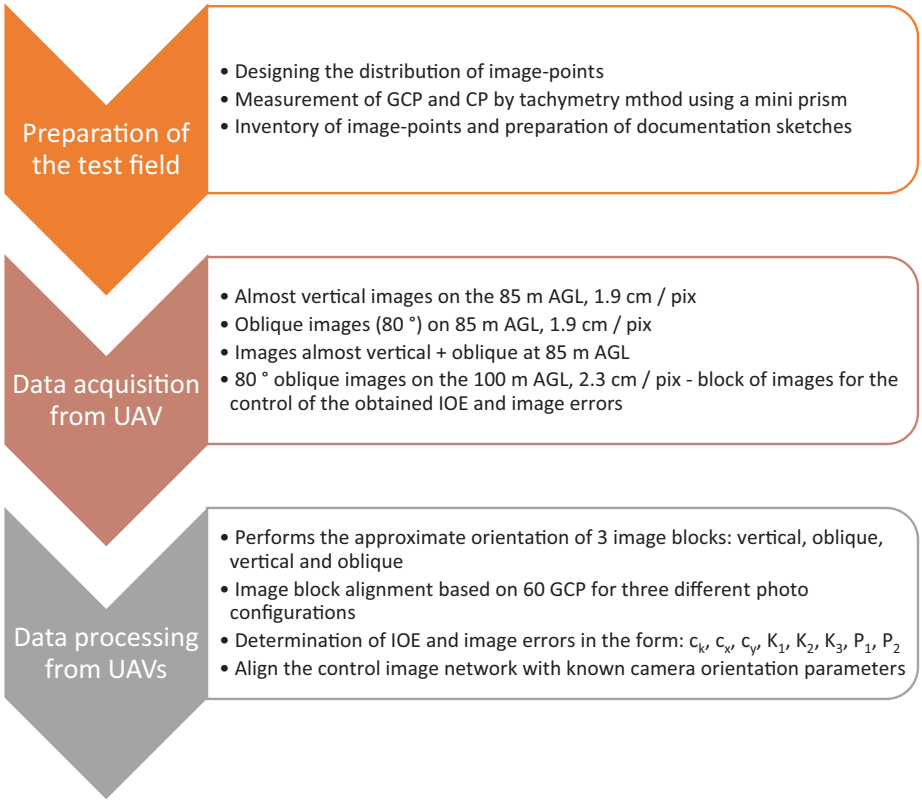

Figure 5. Diagram of the activities carried out in the presented research

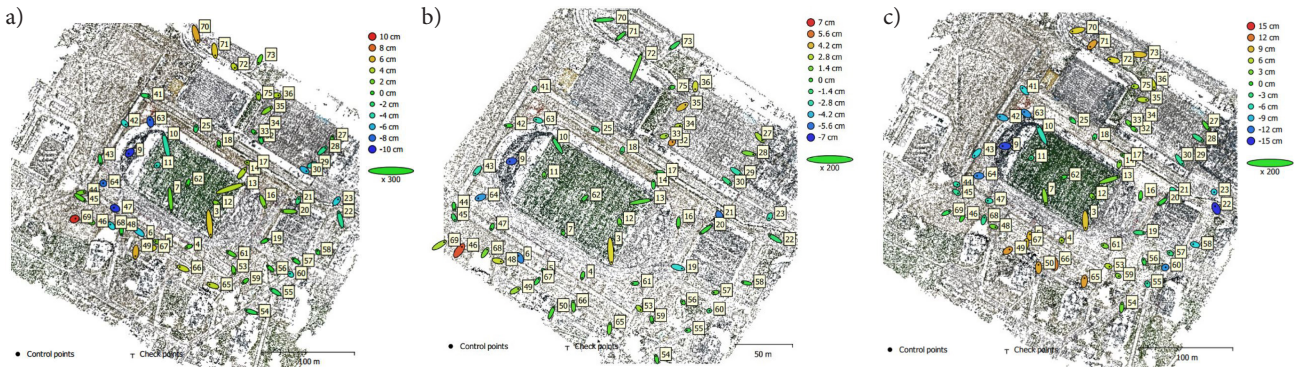

Figure 6. Distribution of model fitting errors on ground control points for the variant: a – vertical images; b – oblique images; c – combination of vertical and oblique images

The quantitative distribution of errors is presented in Table 1. The smallest RMSE error was observed for oblique images, which was 4 cm. XY error values are similar and oscillate around 3 cm. A greater dispersion of error occurs for the Z component.

Figure 7 shows graphs of the differences in the calculated internal orientation elements of the Mavic 2 Pro camera in the form of: the camera constant (Figure 7a) and the coordinates of the principal point (Figure 7b). The greatest difference between the determined ck occurs for the variant of vertical and oblique images, although the values of errors in Table 1 are the largest for the other variant. This may indicate a problem with the stability of the internal orientation elements of the camera.

After running the self-calibration procedure in Agisoft Metashape software, three sets of Mavic 2 Pro UAV camera's internal orientation elements were obtained. Each set concerned a separate configuration of the acquired images. Each set consisted of: camera constant ck, coordinates of the principal point cx and cy, parameters modeling radial distortion K_1, K_2, K_3 and parameters of tangential distortion P_1 and P_2. The obtained results were checked on an independently acquired block.

3.2. Checking the results of the calibration of the UAV camera

In order to check the results obtained for the three analyzed variants of the geometry of the network of images, an additional series of images obtained for the purposes of the inspection was used. Control calculations were performed in Agisoft Metashape software. After importing the images to the project, the camera metric was additionally imported with the first set of internal camera orientation elements, calculated in the previous stage. The imported data in the form of c_k, c_x and c_y, K_1, K_2, K_3 as well as P_1 and P_2 were marked as known data and not

Table 1. Detailed distribution of model fitting errors on ground control points for the analyzed image variants

Configuration of images	Count of GCP	X error (cm)	Y error (cm)	Z error (cm)	XY error (cm)	RMSE (cm)	RMSE (pix)
Vertical	60	1.8	2.4	4.1	3.0	5.1	0.77
Oblique	60	2.5	2.7	2.3	3.7	4.3	1.11
Vertical and oblique	60	2.4	2.4	6.6	3.4	7.4	1.34

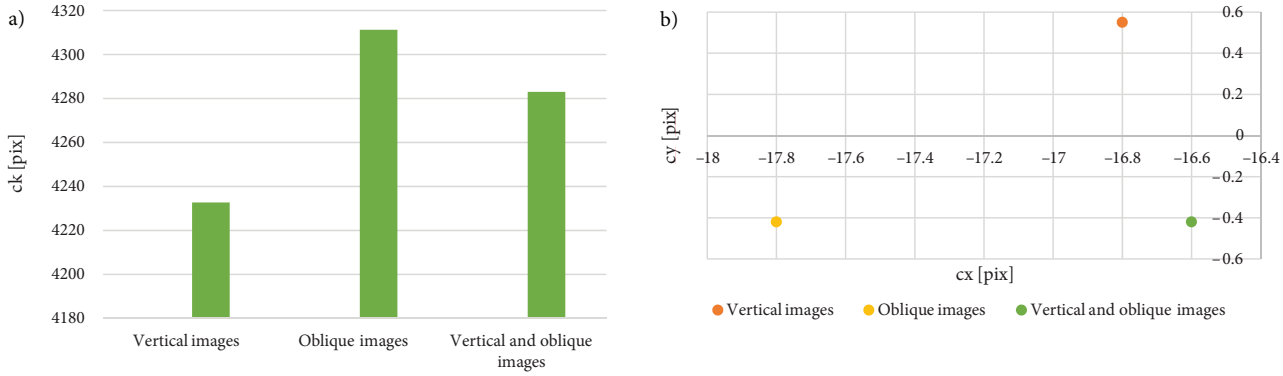

Figure 7. Comparison of the obtained parameters of the camera's internal orientation for the three analyzed variants: a – distribution of changes in the camera constant; b – distribution of changes in the coordinates of the principal point

subject to alignment in the process of aerotriangulation of the photo block with the bundle method. The procedure was repeated for two successive variants of the geometry of the network of photos. In order to fit the model into the metric coordinate system, six of the same, evenly spaced GCP in the area of the experimental training ground were used in each variant. The remaining points on the testing ground were treated as CP (check points). The distribution of errors in fitting the model to ground control points together with the distribution of errors at check points is presented in Table 2 and Table 3.

When analyzing the obtained results, it was observed that importing data from the self-calibration of the UAV camera and setting them as known and not subject to

Table 2. Detailed distribution of model fitting errors on ground control points for the analyzed image variants, assuming the knowledge of the internal orientation elements of the tested Mavic 2 Pro camera

Configuration of images	Count of GCP	X error (cm)	Y error (cm)	Z error (cm)	XY error (cm)	RMSE (cm)	RMSE (pix)
Vertical	6	9.8	4.2	25.4	10.7	27.5	1.45
Oblique	6	1.6	0.9	5.4	1.8	5.7	1.12
Vertical and oblique	6	5.1	2.0	13.9	5.5	14.9	1.01

Table 3. Detailed distribution of model fitting errors at check points for the analyzed image variants, assuming the knowledge of the internal orientation elements of the tested Mavic 2 Pro camera

Configuration of images	Count of CP	X error (cm)	Y error (cm)	Z error (cm)	XY error (cm)	RMSE (cm)	RMSE (pix)
Vertical	41	8.9	6.5	41.6	11.0	43.0	1.06
Oblique	41	3.1	2.9	12.9	4.2	13.5	1.20
Vertical and oblique	41	5.0	4.0	24.5	6.4	25.3	0.85

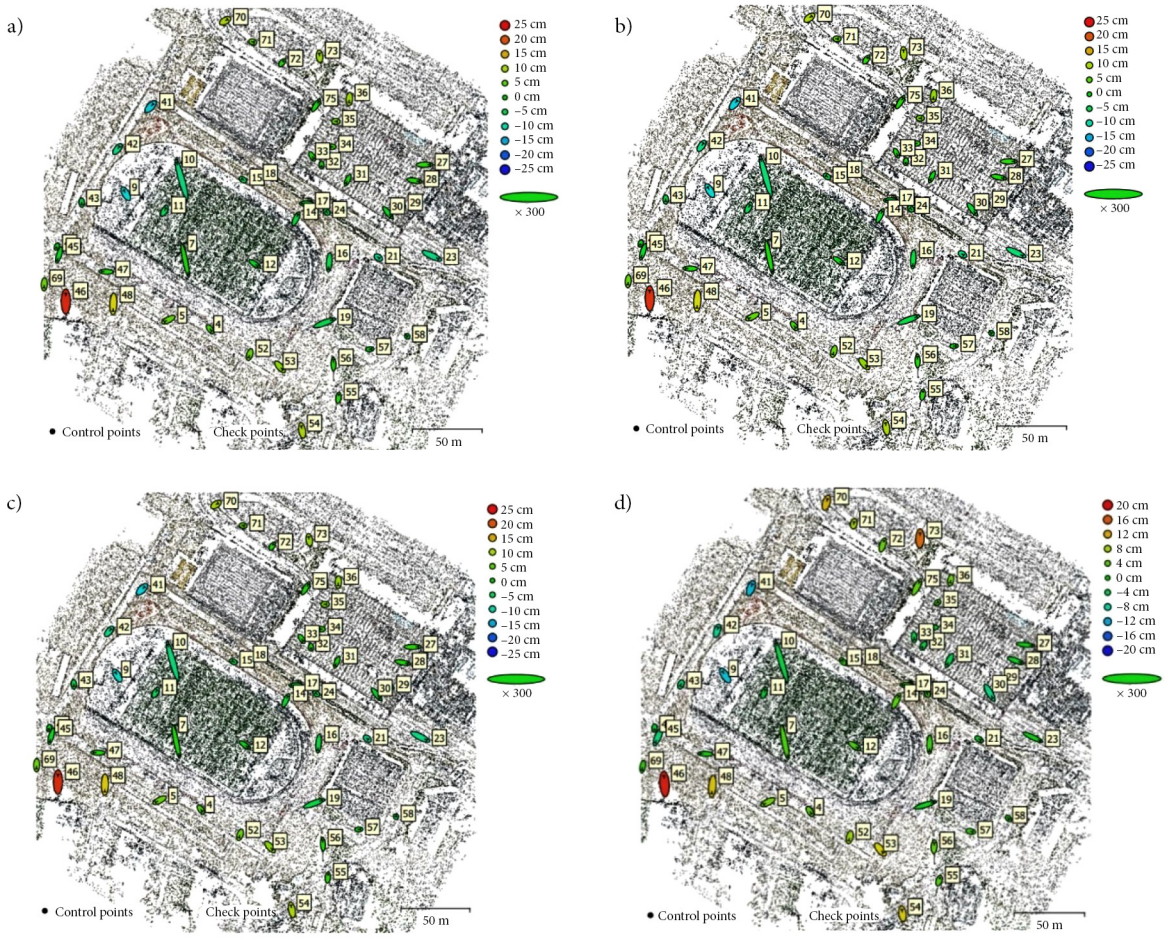

Figure 8. Visualization of the error distribution after aligning the control image block using the obtained elements of internal orientation as exact approximations: a – from almost vertical images; b – oblique; c – almost vertical and oblique; d – without exact IOE approximations

alignment, does not affect the achievement of high accuracy of photogrammetric measurements. Moreover, the applied procedure does not allow to carry out measurements with the accuracy corresponding to the first group of field details suitable in Poland.

It was decided to check whether the obtained results from the calibration of the UAV camera are able to increase the accuracy of the measurements if they are treated as more accurate approximations of the unknown elements of the camera's internal orientation. For comparison, the control block of images from the UAV was aligned – without giving approximations of the internal orientation elements from the previous stage of camera calibration (i.e. using the default approximations suggested in the program where the camera constant ck is equal to the focal length f). This allowed to determine whether performing the calibration procedure of the Mavic 2 Pro UAV camera brings any benefits compared to the standard approach, i.e. simultaneous alignment of the centers of image projections with elements of internal camera orientation and image errors. Figure 8 shows the distribution of errors at control points around the testing ground for the four discussed variants of calculating the elements of internal orientation, i.e. based on the approximations obtained from the previous stage (Figure 8a–c) or without exact approximations (Figure 8d).

In turn, in Table 4 and Table 5 shows errors in fitting the model to ground control points and on check points after aligning the control image block, using the obtained elements of internal orientation as exact approximations from the previous chapter and without giving approximations.

4. Discussion

One of the problems of indirect georeferencing related to absolute orientation is the determination of the optimal number of ground control points. Increasing the amount of GCP usually increases the working time and the cost of the project. Thus, the aim is to minimize the number of GCP, i.e. to determine the number of points for measurements that will allow the spatial model of the study area to fit into the smallest number of GCP points and at the same time ensuring the appropriate precision of the obtained observations (Sobura, 2021). It is worth noting that the amount of GCP depends, among others, on on the features of the mapped area, which means that there are no stable and universal rules regarding the optimal number of image-points to assign indirect georeferencing (Wiącek, 2020). The number of ground control points in the field can be reduced if you have elements of internal orientation of the digital camera.

The metric cameras used in photogrammetry are able to guarantee the stability of the internal orientation elements. The more commonly used non-metric cameras are characterized by instability and ignorance of the elements of internal orientation, i.e. these values are not provided by the manufacturer, therefore it is necessary to calibrate such cameras, e.g. during their operation (Radford & Bevan, 2019; Fryskowska et al., 2016; Bakuła & Ostrowski, 2012). A commonly used solution during post-processing of UAV images is simultaneous aerotriangulation combined with self-calibration of the measuring camera and alignment of observations by the bundle method. Nevertheless, the optimal option would be to have a camera metric, which would reduce the number of unknowns in the collinearity equation and increase the accuracy of the measurement and the speed of the calculations.

In Table 1 shows mean square RMSE errors after fitting the model created on the basis of images into GCP. The highest accuracy was obtained for the configuration of oblique images, which is related to the more advantageous geometry of the network for aerotriangulation. The

Table 4. Visualization of the distribution of errors in fitting the model to GCP after aligning the control image block using the obtained elements of internal orientation as exact approximations and a variant without approximations

Configuration of images	Count of GCP	X error (cm)	Y error (cm)	Z error (cm)	XY error (cm)	RMSE (cm)	RMSE (pix)
Vertical + IOE approximations	6	1.1	0.9	2.0	1.4	2.4	0.84
Oblique + IOE approximations	6	1.1	0.9	2.0	1.4	2.5	0.84
Vertical and oblique + IOE approximations	6	1.1	0.9	1.9	1.4	2.4	0.84
Oblique without approximations	6	1.1	1.3	3.9	1.7	4.2	0.85

Table 5. Visualization of the distribution of errors in fitting the model to CP after aligning the control image block using the obtained elements of internal orientation as exact approximations and a variant without approximations

Configuration of images	Count of CP	X error (cm)	Y error (cm)	Z error (cm)	XY error (cm)	RMSE (cm)	RMSE (pix)
Vertical + IOE approximations	41	1.4	2.3	7.3	2.7	7.7	0.83
Oblique + IOE approximations	41	1.4	2.3	7.1	2.7	7.6	0.83
Vertical and oblique + IOE approximations	41	1.4	2.3	7.1	2.7	7.6	0.83
Oblique without approximations	41	1.5	2.4	6.7	2.8	7.2	0.83

calculated three variants of the internal orientation elements of the Mavic 2 Pro camera were used in the next stage of the research, checking the quality of the obtained models in an additional control block of images. In the first stage of the control, the tested parameters were found to be stable and constant, i.e. they were not adjusted by the bundle method in the process of aerotriangulation. The results from this stage are presented in Tables 2 and 3. The mp_{XYZ} errors at over forty control points ranged from 14 to 43 cm, and the obtained values were considered too large for geodetic measurements. This meant that the adopted assumption about the stability of the elements of the internal orientation of the analyzed camera was incorrect. In the second stage, it was checked whether treating the obtained results from the camera calibration as an exact approximation of the searched parameters improves the quality of the network and the accuracy of the measurements. A comparative variant was the classic UAV image development approach, i.e. where the approximations of the internal orientation elements are unknown (they are zero and the camera constant is equal to the focal length). The use of more precise approximations of the elements of internal orientation had a positive effect on the accuracy of fitting the model to the ground control points, as shown in tab. 4. Unfortunately, the better quality of the model did not significantly affect the accuracy of the measurements, where the mp_{XYZ} errors on the control points – regardless of the geometry of the network from the images and the approximations used – were about 7 cm.

The current technical standards in Poland allow for methods and measurement technologies that meet certain accuracy criteria for geodetic measurements. The most common evidence that the above-mentioned criteria are met is the accuracy analysis included in the technical report in the survey. This means that the source of obtaining observations for measurements can be not only aerial images taken with a professional photogrammetric camera, but also very popular images from unmanned aerial vehicles, provided that the accuracy requirements are met (Pyka & Myszka, 2015). Performing a UAV flight over a spatial test field, intended for the calibration of optical cameras, allows you to check the real accuracy of photogrammetric measurements for various groups of field details.

Conclusions

For the analyzed non-metric camera of the Mavic 2 Pro unmanned aerial vehicle, the use of camera calibration results on a properly prepared test field does not allow to increase the accuracy of photogrammetric studies (Table 5). The reason for this is probably the instability of the autofocus, and thus the problem with the repeatability of determining the elements of internal orientation of the analyzed UAV camera. Despite turning off the autofocus system during the acquisition of images, the fixed camera could have been changed during the replacement of the battery in the UAV. The optimal solution would be to use lenses with a focusing ring and blocking the ring during measurements. Unfortunately, in non-professional drones such a solution is not provided for. Treating the results of the camera calibration as good quality approximations of the elements of internal orientation favors a faster and more accurate creation of a spatial model in the form of a sparse points cloud (Table 4).

On the basis of the conducted research, the authors concluded that there are many benefits of designing a testing ground for the calibration of UAV cameras. Testing the unmanned aerial vehicle over a spatial test field allows to determine the real accuracy of the photogrammetric measurements for various types of objects and various image configurations. This can be of assistance to surveying companies that need to test low altitude photogrammetry for specific applications.

References

Aldelgawy, M., & Abu-Qasmieh, I. (2021). Calibration of smartphone's rear dual camera system. *Geodesy and Cartography*, *47*(4), 162–169. https://doi.org/10.3846/gac.2021.13434

Bakuła, K., & Ostrowski, W. (2012). The application of non-metric digital camera in aerial photogrammetry on selected examples. *Archiwum Fotogrametrii, Kartografii i Teledetekcji*, *24*, 11–20.

Cramer, M., Przybilla, H.-J., & Zurhorst, A. (2017). UAV cameras: Overview and Geometric Calibration Benchmark. *The International Archives of Photogrammetry, Remote Sensing Spatial Information Sciences*, *XLII-2/W6*, 85–92. https://doi.org/10.5194/isprs-archives-XLII-2-W6-85-2017

Fryskowska, A., Kedzierski, M., Grochala, A., & Braula, A. (2016). Calibration of low cost RGB and NIR UAV cameras. *The International Archives of the Photogrammetry, Remote Sensing and Spatial Information Sciences*, *XLI-B1*, 817–821. https://doi.org/10.5194/isprsarchives-XLI-B1-817-2016

Łojek, M., & Łyjak, D. (2022). *Kalibracja kamer UAV na terenowym polu testowym* [master thesis]. Politechnika Świętokrzyska, Kielce (in Polish).

Oniga, V.-E., Pfeifer, N., & Loghin, A.-M. (2018). 3D Calibration test-field for digital cameras mounted on Unmanned Aerial Systems (UAS). *Remote Sensing*, *10*(12), 2017. https://doi.org/10.3390/rs10122017

Pérez, M., Agüera, F., & Carvajal, F. (2011). Digital camera calibration using images taken from an unmanned aerial vehicle. *The International Archives of the Photogrammetry, Remote Sensing and Spatial Information Sciences*, *XXXVIII-1/C22*, 167–171. https://doi.org/10.5194/isprsarchives-XXXVIII-1-C22-167-2011

Pyka, K., & Myszka, P. (2015). Status fotogrametrii w ustawie prawo geodezyjne i kartograficzne i przepisach powiązanych. *Archiwum Fotogrametrii, Kartografii i Teledetekcji*, *27*, 97–107 (in Polish). https://doi.org/10.14681/afkit.2015.007

Radford, C. R., & Bevan, G. (2019). A calibration workflow for "prosumer" UAV cameras. *The International Archives of the Photogrammetry, Remote Sensing and Spatial Information Sciences*, *XLII-2/W13*, 553–558. https://doi.org/10.5194/isprs-archives-XLII-2-W13-553-2019

Sampath, A., Moe, D., & Christopherson, J. (2012). Two methods for self calibration of digital camera. *International Archives of the Photogrammetry, Remote Sensing and Spatial Information Sciences*, *XXXIX-B1*, 261–266. https://doi.org/10.5194/isprsarchives-XXXIX-B1-261-2012

Sobura, S. (2021). Calibration of non-metric UAV camera using different test fields. *Geodesy and Cartography*, *47*(3), 111–117. https://doi.org/10.3846/gac.2021.13080

Tokarczyk, R. (2022, September 20). *Kalibracja kamer bliskiego zasiegu* [slides]. Faculty of Mining Surveying and Environmental Engineering, AGH University of Science and Technology (in Polish). https://www.yumpu.com/xx/document/view/47489720/kalibracja-kamer-bliskiego-zasiagu-agh

Tokarczyk, R., & Boroń, A. (2020). Badanie cyfrowych aparatów fotograficznych dla zastosowań fotogrametrycznych. *Archiwum Fotogrametrii, Kartografii i Teledetekcji*, *10*, 63-1–63-10 (in Polish).

Wiącek, P., & Pyka, K. (2019). The test field for UAV accuracy assessments. *The International Archives of the Photogrammetry, Remote Sensing and Spatial Information Sciences*, *XLII-1/W2*, 67–73. https://doi.org/10.5194/isprs-archives-XLII-1-W2-67-2019

Wiącek, P. (2020). The database for multifactorial UAV accuracy assessments. *The International Archives of the Photogrammetry, Remote Sensing and Spatial Information Sciences*, *XLIII-B5-2020*, 163–172. https://doi.org/10.5194/isprs-archives-XLIII-B5-2020-163-2020